Published in final edited form as:
J Diabetes Sci Technol. 2009 March 1; 3(2): 297–303. doi:10.1901/jaba.2009.3-297.

A Nanoporous, Transparent Microcontainer for Encapsulated Islet Therapy

Barjor Gimi, Ph.D.[1,2,3], **Joonbum Kwon**[2], **Andrey Kuznetsov, M.S.**[4], **Behroze Vachha, M.D., Ph.D.**[1], **Richard L. Magin, Ph.D.**[3], **Louis H. Philipson, M.D., Ph.D.**[4], and **Jeong-Bong Lee, Ph.D.**[2]

[1]The University of Texas Southwestern Medical Center, Dallas, Texas

[2]University of Texas at Dallas, Dallas, Texas

[3]University of Illinois at Chicago, Chicago, Illinois

[4]University of Chicago, Chicago, Illinois

Abstract

Present-day islet encapsulation techniques such as polymer microcapsules and microelectromechanical system (MEMS)-based biocapsules have shown promise in insulin replacement therapy, but they each have limitations—the permeability characteristics of existing polymeric capsules cannot be strictly controlled because of tortuosity and the large size of present-day MEMS biocapsules leads to necrotic regions within the encapsulation volume. We report on a new microcontainer to encapsulate and immunoprotect islets/β cells that may be used for allo- or xenotransplantation in cell-based therapy. The microcontainers have membranes containing nanoslots to permit the bidirectional transport of nutrients, secretagogues, and cellular products while immunoprotecting the encapsulated cells. The 300-μm microcontainers were fabricated from an epoxy-based polymer, SU-8, with 50-μm-thick walls. Arrays of 25-nm wide slots were created in the SU-8 microcontainer lid. Isolated mouse islets were encapsulated in the microcontainer, and their physiological response to glucose was studied with fluorescence and two-photon imaging over 48 hours. The physiological response of the encapsulated islets was indistinguishable from controls. An agarose-filled microcontainer was imaged with magnetic resonance imaging to demonstrate the feasibility of future noninvasive, *in vivo* imaging. The SU-8 microcontainers maintained mechanical integrity upon islet loading and mechanical manipulation. Islet encapsulation, as well as the ability to visualize islet function within these transparent microcontainers, was demonstrated.

Keywords

cell encapsulation; cell encapsulation therapy; cell therapy; immunoisolation; immunoprotection; microcontainers

Introduction

Encapsulated cell therapy can alter or restore endogenous function and has potential use in myriad diseases.[1–7] Transplanted islets have been used in insulin replacement therapy for type 1 diabetes.[3] As opposed to exogenous insulin sources, transplanted islets secrete insulin as a

Corresponding Author: Barjor Gimi, Ph.D., The University of Texas Southwestern Medical Center, 5323 Harry Hines Boulevard, Dallas, TX 75390-9058; barjorg@yahoo.com.

graded response to host glucose levels, more closely mimicking normal pancreatic function, and can minimize many postoperative complications of organ (pancreas) transplantation. Islet xenotransplantation can potentially overcome the severe shortage of human islets available for grafting. Effective immunoisolation of these xenografts can avoid a lifelong requirement of immunosuppressive drugs, which has deleterious effects on β-cell function and on the host's ability to combat disease. Therefore, several researchers have focused on strategies to encapsulate islets so as to immunoisolate them for grafting.[8,9]

Despite the potential advantages of encapsulated islet therapy, its clinical potential has not been realized with current encapsulation schemes. Microcapsules made from polymers such as alginate and hydroxyethyl methacrylate–methyl methacrylate are most prevalent in cell encapsulation therapy,[5,10,11] but these polymers have a wide distribution of pore sizes, which in turn allows some immune complement compounds to enter the microcapsule and destroy the encapsulated cells.[12] Microelectromechanical system (MEMS)-based biocapsules, comprising polymer capsules with nanoporous silicon membranes bonded to their surface, however, have precise nanometer-scale control over membrane porosity, but these biocapsules are on the order of several millimeters and therefore are not sufficiently small to be implanted in many desirable locations such as within the microvasculature of highly immunoprivileged sites or into frequently employed sites such as the liver and renal subcapsule.[12] Similarly, recently developed polyethylene glycol hydrogels have demonstrated facile control over porosity, but the microbeads so formed are large and present a barrier to rapid molecular transport.[13]

To address the aforementioned challenges associated with present-day islet encapsulation strategies, we present a new generation of microencapsulation devices: epoxy-based polymer microcontainers that can be introduced through portal infusion or otherwise dispersed at desired transplant sites in the body. The cross-linked epoxy polymer should prevent the passage of antibodies and complement molecules. The surface porosity and the small size of the microcontainer, with a 200 × 200 × 200-μm^3 (8 nl) encapsulation volume, provide adequate nutrients and oxygen to the encapsulated islet. To facilitate the post-transplantation imaging of islet viability and function, we designed microcontainers that were optically and magnetic resonance imaging (MRI) transparent.

Methods

Microcontainer Fabrication

The microcontainer has two components—a hollowed cubic base (Figure 1) for encapsulating cells and a nanoporous lid (Figure 2) that seals the device after it is filled with its cellular payload. The microcontainer was fabricated using the highly cross-linked, epoxy-based polymer SU-8, which is characterized by a high glass transition temperature (210°C), thermal stability (315°C at 5% weight loss), a tensile strength of 60 MPa, and a Young's modulus of 2 GPa.

The fabrication process for the hollowed cubic base began with a 300-Å chromium (Cr) adhesion layer deposition on a Pyrex wafer using electron (E)-beam evaporation or sputtering. Next, an Omnicoat (Microchem, Newton, MA) adhesion layer and a 50-μm-thick SU-8 2025 photoresist (Microchem) layer were spun on the wafer. This layer of SU-8 was patterned to form the bottom face of the hollowed cubic base. Finally, a 250-μm-thick layer of SU-8 2075 was spun on the patterned 50-μm-thick SU-8 bottom face, planarized, baked, and patterned to form the four side walls of the hollowed cubic base.

The microcontainer lid comprises multiple SU-8 islands of a 500-nm-thin membrane patterned in 30-μm-thick SU-8 (Figures 3b and 3c). The fabrication sequence for the microcontainer lid

began with deposition of a 300-Å Cr adhesion layer by E-beam evaporation or sputtering on an oxidized silicon wafer. Copper (Cu) alignment marks, 200 Å thick, were formed on top of the Cr-coated wafer using a lift-off process. Next, an Omnicoat adhesion layer and 500-nm-thin SU-8 2000.5 were spun and patterned to form thin islands for future milling of a nanoslot array. In addition, 30-μm-thick SU-8 2010 was spun and patterned to form the lid. Finally, the SU-8 lids were released from the oxidized silicon wafer by wet etching of the oxide layer, and the Cu alignment marks were removed by a Cu etchant. The microcontainer base and lid were both flood exposed to ensure near complete SU-8 cross-linking.

The lid, lifted from the oxidized silicon wafer, was further processed by a focused ion beam (FIB) to form a nanoslot array in the thin SU-8 islands (Figure 3c). The lid was coated with a 150-Å-thick Cr layer, which eliminates charging in the SU-8 film during FIB milling. Multiple nanoslots as small as 25 nm in width were drilled using FIB (FEI Nova 200 NanoLab) with an applied voltage of 30 kV, a current of 10 pA, a dwell time of 1 μs.

Islet Isolation and Culture

All our islet work and use of animals were approved by our animal care committee—in this case, University of Chicago IACUC protocol 71492 (mouse) (reapproval date 11/03/2008).

Islets were isolated from the pancreata of 1- to 5-month-old C57BL/6 mice (The Jackson Laboratory, Bar Harbor, ME) using collagenase digestion and Ficoll gradients as described previously.[14] Isolated islets were cultured in Roswell Park Memorial Institute 1640 medium supplemented with 10% fetal calf serum, 100 U/ml penicillin, and 100 μg/ml streptomycin in a humidified incubator at 37°C under an atmosphere of 95% air/5% CO_2.

Islet Encapsulation

The microcontainers and lids were autoclaved, and all experiments were performed under sterile conditions. Microcontainers were anchored to the glass surface of Matek culture dishes using 5% agarose gel made in phosphate-buffered saline. After allowing 16 hours for the islets to recover postisolation, individual islets were introduced into the microcontainers using an automatic pipette with a sterile long gel-loading tip; one islet was encapsulated per microcontainer. Islets were loaded in fluid phase to ensure the absence of air bubbles within the microcontainer. Islets were then cultured in these encapsulated conditions for 48 hours as described earlier, and their structure, viability, and physiological responses to glucose were studied. Lids were placed using microforceps and anchored using biocement for diffusion chambers (www.millipore.com) and capillary forces.

Magnetic Resonance Microscopy (MRM)

To demonstrate the feasibility of MRM of the interior space of the microcontainers, a microcontainer was embedded in agarose gel and placed in a custom-made SU-8 well that was 350 μm deep and had a 40-μm SU-8 membrane base. This SU-8 well was placed on Bruker 1000/1300-mm inner diameter/outer diameter spiral, radio frequency (RF), surface microcoil detectors (Bruker BioSpin, Switzerland) and imaged with MRM at 500 MHz using a Bruker Micro5 microimaging probe. Images were acquired using a spin echo sequence with a field of view of 0.345 × 0.2 cm, an acquisition matrix of 256 × 192, three contiguous slices 150 μm thick, an echo time of 10 ms, a repetition time of 1200 ms, and 60 signal averages.

Intracellular Ca^{2+} Measurements

Experiments were performed in modified Krebs–Ringer solution (KRH) containing (in mmol/liter) 119 NaCl, 2 $CaCl_2$, 4.7 KCl, 20 HEPES, 1.2 $MgSO_4$, and 1.2 KH_2PO_4 adjusted to pH 7.3 with NaOH and supplemented with glucose to the required concentration. Unencapsulated

controls and encapsulated mouse islets were loaded with 5 μ*M* Fluo-4 AM in KRH with 2 m*M* glucose (KRH2) for 45 minutes at 37°C. The staining solution was replaced with KRH2, and glass-bottom Matek culture dishes with loaded islets were placed in a temperature controller (TC-202, Medical Systems Corp., Greenvale, NY) mounted on the stage of an inverted microscope (Olympus IX70, Olympus America Inc., Center Valley, PA) for imaging. Experiments were carried out at 37°C in static conditions; KRH solutions with different supplements were added and replaced manually. Confocal imaging was performed with a custom-built system based on a Yokogawa CSU10 spinning disk confocal unit. The indicator was excited with the 488-nm line of an argon/krypton laser (Series 43, Omnichrome, Melles Griot, Carlsbad, CA), and the emitted light was passed through a 530/30 filter (Chroma, Rockingham, VT) and recorded with a CoolSNAP HQ digital camera (Roper Scientific, Tucson, AZ). Acquisition was controlled with MetaMorph software (Molecular Devices, Sunnyvale, CA). Leica SP5 AOBS spectral two-photon confocal microscope images of calcium fluxes were also acquired (Leica). Data analysis was performed with MetaMorph and Microsoft Excel. Results were plotted as a time series of calcium fluctuations plotted as changes in Fluo-4 fluorescence as described later.

Two-Photon Imaging

To reduce autofluorescence of the nanoporous microcontainer and improve the temporal resolution of the recordings as compared with conventional confocal microscopy, we measured the intracellular Ca^{2+} changes of an encapsulated islet in response to glucose and tetraethylammonium (TEA) stimulations with a Leica SP5 AOBS spectral two-photon confocal microscope. A Mai Tai® (Newport Corporation, Irvine, CA) pulsed laser tuned to 914 nm was used to excite the Ca^{2+} Fluo-4 indicator through the resonant galvanometer high-speed scanner, and the emitted light collected in the 510- to 550-nm emission window was measured with the internal photomultiplier tube detector at 20 fps.

Results

Physical Characterization of Transparent Microcontainers

The parallel fabrication process resulted in several hundred microcontainers (Figure 1) and lids (Figure 2) from a single process run. While some microcontainers occasionally dissociated from the wafer, most microcontainers remained anchored, resulting in a high yield (>95%). The dimensions of the thin islands of the lid were highly reproducible (within 5%), as were the dimensions of the nanoslots (Figure 3). The microcontainers and lids maintained mechanical integrity upon islet loading, placement of the lid, and mechanical manipulation; there was no shear between the SU-8 2025 and the SU-8 2075 layers of the microcontainer base.

Microcontainers and Encapsulated Islets Are Visualized Easily with Optical Techniques

The microcontainers were optically transparent (Figures 4a and 4b), and the encapsulated islets were visualized easily with confocal imaging (Figure 4b). Confocal imaging allowed for good optical separation of the islet-derived and microcontainer-derived signals, thus making possible functional and structural studies demonstrated here.

Validation of Noninvasive Imaging of Microcontainers Using Magnetic Resonance Microscopy

The custom-made thin SU-8 membrane base of the sample well ensured that the microcontainer was in close proximity to the microcoil detector in MRM so as to obtain a high signal-to-noise ratio during imaging. The interior of the microcontainer was clearly visible in MRM, shown

here in the side view, and the microcontainer boundaries did not reveal any image distortion that would preclude effective MRM of islets within their interior space (Figure 4c).

Islet Encapsulation in Microcontainers Does Not Impair Islet Function

At the end of the 48-hour period, islets appeared anchored to the microcontainer; when observed under a microscope, upon mechanical agitation of the tissue culture dish, which resulted in considerable motion in the medium, islets appeared immobile. When assessed by changes in the concentration of intracellular Ca^{2+}, responses of the encapsulated islets to physiologically elevated glucose (KRH with 14 m*M* glucose, KRH14) and to a combination of the elevated glucose (KRH14) with the potent potassium channel inhibitor TEA (20 m*M*) were undistinguishable from the responses of normal mouse islets from the same batch of isolation. A representative trace for an encapsulated islet is shown in Figure 5. Similar traces obtained for control islets and two-photon data are not shown.

Discussion

This work describes a new design for a cell encapsulation device that is optically and MRI transparent with precise and reproducible surface porosity. The surface porosity and small size of the microcontainer should allow adequate oxygenation and nutrient support to the encapsulated cells.[15]

Lanza and colleagues[16] have shown the retention of immunoglobulin and complement molecules by membranes with a maximum pore diameter of 30 nm; our epoxy-based microcontainer was designed to prevent the passage of immune complement components based on pore size exclusion.[12] While we report a pore size of 25 nm for our microcontainers, our innovative fabrication allows us to create more uniform and much deeper pores than those used in previous generations of biocapsules, which should increase impedance to molecular transport and aid in the pore-size exclusion of molecules. It is noteworthy that proteins do not have a fixed conformation but can assume several energetically allowable states. Iwata and associates[17] have shown that complements are inactivated upon passage through a membrane. Therefore, the goal may not be to merely prevent the passage of molecules, but rather ensure that complements are inactivated upon transport through the membrane. We will study this issue further and optimize membrane architecture and pore depth to validate our system.

The microcontainers are devised to protect the encapsulated islets from the stresses experienced during and after transplantation. The microcontainers used in this study were mechanically robust and did not fracture or rupture when manipulated during manufacture and encapsulation. This represents an improvement over alginate-based microcapsules, which rupture due to mechanical instability, as well as present-day MEMS-based biocapsules, which are prone to rupture because of the large surface area of their thin membranes. Furthermore, these MEMS-based biocapsules are still too large for implantation at sites other than the peritoneal cavity or subcutaneously, which severely impedes vascular access to the encapsulated cells. Our miniaturization strategy, along with recessed islands to protect the permselective membrane, resulted in mechanically robust encapsulation devices that did not deform or rupture.

Miniaturization of the encapsulation device also provides a large surface area to volume ratio, and the 200 × 200 × 200-μm^3 (8 nl) encapsulation volume allows for adequate oxygenation of the encapsulated cells so as to prevent hypoxia and necrosis.[15] Additionally, device miniaturization should also permit implantation of our microcontainers at sites that are problematic or preclude larger biocapsules and hydrogel microcapsules. Our microcontainers should therefore allow us to revisit sites such as the liver, the renal subcapsule, spleen, or elsewhere within the host and should enable future evaluation of optimal ectopic sites for islet grafts. Microcontainer implantation within immune-privileged and highly vascularized sites

could provide a long-term or permanent source of therapy and may reduce or eliminate the necessity for multiple grafting.

Among the key features of our microcontainer design are optical and MRI transparency. This transparency permits multimodal imaging of encapsulated islets post-transplantation. Optical transparency allows visualization of the encapsulated islets, as well as the evaluation of their viability and function using functional dyes and fluorophores. We are developing transgenic mice expressing several fluorescent biosensor molecules in their β cells. These biosensors are designed for reporting a number of crucial physiological parameters of β cells, such as intracellular Ca^{2+} and redox state. We plan to use islets isolated from these animals for encapsulation and subsequent transplantation in donor mice. *In vivo* studies are possible using two-photon confocal microscopy, providing the most efficient means of recording the signals of the biosensor after transplantation, allowing us to directly study their survival and physiology *in situ*.

The MRI transparency of the microcontainers described here is a considerable advance over MRI-opaque microcontainers, which can be traced noninvasively but preclude direct imaging of the encapsulated cells owing to the RF shielding effect.[18] The spiral, microcoil RF detector provides the ultrahigh resolution required to image the interior volume of the microcontainers using MRM. The ~10-μm in-plane image resolution enables MRM at single cell resolution. Such microcoils, integrated with the microcontainer, can provide noninvasive and multiparametric information of encapsulated cell viability and function, *in vivo* and post-transplantation.[19] Additionally, the ability to observe the interior space of the microcontainers noninvasively makes it feasible to evaluate its cellular contents functionally using the differential contrast uptake of Mn^{2+} for MRI of islet function.[20]

Encapsulated islet survival and function for 48 hours provide evidence that the microcontainers are not toxic under these experimental conditions. Intracellular calcium fluxes of the encapsulated islets are comparable to unencapsulated controls. While previous work has sought to establish the biocompatibility of SU-8, further biocompatibility testing is necessary as we move toward preclinical studies.[21] If necessary, subsequent to preclinical testing, the SU-8 surfaces of the microcontainer can be coated easily with biofriendly molecules or with bioinert materials such as gold.

While hydrogel microcapsules have a larger surface area, which allows for more diffusion of glucose and nutrients, the thin island structures within our microcontainers should result in the rapid molecular transport of nutrients and secretagogues such as glucose, unlike the larger diffusion barriers of up to several micrometers as encountered with alginate encapsulation.[22]

In an earlier report, Gimi and colleagues[18] demonstrated the utility of self-assembled MEMS-based microcontainers for cell encapsulation and MRI tracking. The new generation of microcontainers presented here provides several advantages over the self-assembled microcontainers. First, the encapsulation volume of our microcontainers is assembled prior to cell loading, and therefore cell loading occurs in a biofriendly environment, whereas the self-assembled microcontainers, in their current form, require exposure to harsh chemicals and high temperatures for assembly, thereby precluding cell loading except in the case of open-surface microcontainers. Second, our new layered assembly process eliminates the risk of overfolding or underfolding of the encapsulation devices, as was the case with self-assembled microcontainers. Third, the process allows easy nanopore and nanoslot formation, unlike the thick, metallic self-assembled microcontainers. Finally, this generation of microcontainers is optically and MRI transparent, allowing for multimodality *in vivo* imaging of encapsulated cell fate and function.

While the results obtained with our islet-encapsulating microcontainers are encouraging and warrant further *in vitro* and *in vivo* investigation, our system needs to be expanded and extended for preclinical use. Ongoing studies are focused on optimizing surface nanoporosity, increasing the efficiency of nanopore formation and the high throughput loading of islets using a microneedle array, automating the process of placing and securing the lids, and characterizing the postimplantation biocompatibility and mechanical stability of the microcontainers and long-term *in vivo* graft survival and function.

Conclusions

We have devised an islet encapsulation device to overcome the challenges of present-day encapsulation techniques. The small size of the microcontainer supports the survival of encapsulated islets and enables access to various implant sites deep within the body so as to enable their highly localized implantation.

We envision that optical and MRI assessments of encapsulated islets will assist in early identification of the loss of graft function and may direct strategies for rescuing and replenishing grafts, help in dosing of immunosuppressive regimens, and identify optimal transplant sites. Our strategy can be adapted easily to encapsulate β/islet cells or other cells that secrete biotherapeutic molecules.

Abbreviations

Cu, copper; E, electron; FIB, focused ion beam; KRH, Krebs–Ringer solution; MEMS, microelectromechanical system; MRI, magnetic resonance imaging; MRM, magnetic resonance microscopy; RF, radio frequency; TEA, tetraethylammonium.

Acknowledgments

This work was supported by NIH R01 EB007456 and P60 DK-20595 NIH DRTC support from the Islet Biology Core laboratory. We thank Dr. Robert Kleps of the Research Resources Center at the University of Illinois at Chicago for assistance with MRI.

References

1. Aebischer P, Tresco PA, Winn SR, Greene LA, Jaeger CB. Long-term cross-species brain transplantation of a polymer-encapsulated dopamine-secreting cell line. Exp Neurol 1991;111(3):269–275. [PubMed: 1999230]
2. Chang TM. Semipermeable microcapsules. Science 1964;146:524–525. [PubMed: 14190240]
3. O'Shea G, Sun A. Encapsulation of rat islets of Langerhans prolongs xenograft survival in diabetic mice. Diabetes 1986;35(8):943–946. [PubMed: 3089856]
4. Sagot Y, Tan SA, Baetge E, Schmalbruch H, Kato AC, Aebischer P. Polymer encapsulated cell lines genetically engineered to release ciliary neurotrophic factor can slow down progressive motor neuronopathy in the mouse. Eur J Neurosci 1995;7(6):1313–1322. [PubMed: 7582105]
5. Uludag H, Sefton MV. Microencapsulated human hepatoma (HepG2) cells: *in vitro* growth and protein release. J Biomed Mater Res 1993;27(10):1213–1224. [PubMed: 8245036]
6. Orive G, Hernández RM, Gascón AR, Calafiore R, Chang TM, De Vos P, Hortelano G, Hunkeler D, Lacík I, Shapiro AM, Pedraz JL. Cell encapsulation: promise and progress. Nat Med 2003;9(1):104–107. [PubMed: 12514721]
7. Gimi, B.; Kwon, J.; Kuznetsov, A.; Vachha, B.; Philipson, LH.; Lee, JB. Islet encapsulation in epoxy-based microcontainers. Proceedings of the 7th annual Diabetes Technology Society; 2007 Oct; San Francisco.
8. Kizilel S, Garfinkel M, Opara E. The bioartificial pancreas: progress and challenges. Diabetes Technol Ther 2005;7(6):968–985. [PubMed: 16386103]

9. Beck J, Angus R, Madsen B, Britt D, Vernon B, Nguyen KT. Islet encapsulation: strategies to enhance islet cell functions. Tissue Eng 2007;13(3):589–599. [PubMed: 17518605]
10. Visted T, Bjerkvig R, Enger PO. Cell encapsulation technology as a therapeutic strategy for CNS malignancies. Neuro Oncol 2001;3(3):201–210. [PubMed: 11465401]
11. Rihova B. Immunocompatibility and biocompatibility of cell delivery systems. Adv Drug Deliv Rev 2000;42(1–2):65–80. [PubMed: 10942815]
12. Desai TA, West T, Cohen M, Boiarski T, Rampersaud A. Nanoporous microsystems for islet cell replacement. Adv Drug Deliv Rev 2004;56(11):1661–1673. [PubMed: 15350295]
13. Weber LM, Cheung CY, Anseth KS. Multifunctional pancreatic islet encapsulation barriers achieved via multilayer PEG hydrogels. Cell Transplant 2007;16(10):1049–1057. [PubMed: 18351021]
14. Philipson LH, Rosenberg MP, Kuznetsov A, Lancaster ME, Worley JF 3rd, Roe MW, Dukes ID. Delayed rectifier K+ channel overexpression in transgenic islets and beta-cells associated with impaired glucose responsiveness. J Biol Chem 1994;269(45):27787–27790. [PubMed: 7961701]
15. Thomlinson RH, Gray LH. The histological structure of some human lung cancers and the possible implications for radiotherapy. Br J Cancer 1995;9(4):539–549. [PubMed: 13304213]
16. Lanza RP, Sullivan SJ, Chick WL. Perspectives in diabetes: islet transplantation with immunoisolation. Diabetes 1992;41(12):1503–1510. [PubMed: 1446791]
17. Iwata H, Morikawa N, Fujii T, Takagi T, Samejima T, Ikada Y. Does immunoisolation need to prevent the passage of antibodies and complement? Transplant Proc 1995;27(6):3224–3226. [PubMed: 8539926]
18. Gimi B, Artemov D, Leong T, Gracias DH, Gilson W, Stuber M, Bhujwalla ZM. Cell viability and noninvasive *in vivo* MRI tracking of 3D cell encapsulating self-assembled microcontainers. Cell Transplant 2007;16(4):403–408. [PubMed: 17658130]
19. Gimi B, Eroglu S, Leoni L, Desai TA, Magin RL, Roman B. NMR spiral surface microcoils: applications. Concepts Magn Resonance Imag Part B Magn Resonance Engin 2003;18B(1):1–8.
20. Gimi B, Leoni L, Oberholzer J, Braun M, Avila J, Wang Y, Desai T, Philipson LH, Magin RL, Roman BB. Functional MR microimaging of pancreatic beta-cell activation. Cell Transplant 2006;15(2): 195–203. [PubMed: 16719054]
21. Voskerician G, Shive MS, Shawgo RS, von Recum H, Anderson JM, Cima MJ, Langer R. Biocompatibility and biofouling of MEMS drug delivery devices. Biomaterials 2003;24(11):1959–1967. [PubMed: 12615486]
22. Wyman JL, Kizilel S, Skarbek R, Zhao X, Connors M, Dillmore WS, Murphy WL, Mrksich M, Nagel SR, Garfinkel MR. Immunoisolating pancreatic islets by encapsulation with selective withdrawal. Small 2007;3(4):683–690. [PubMed: 17340661]

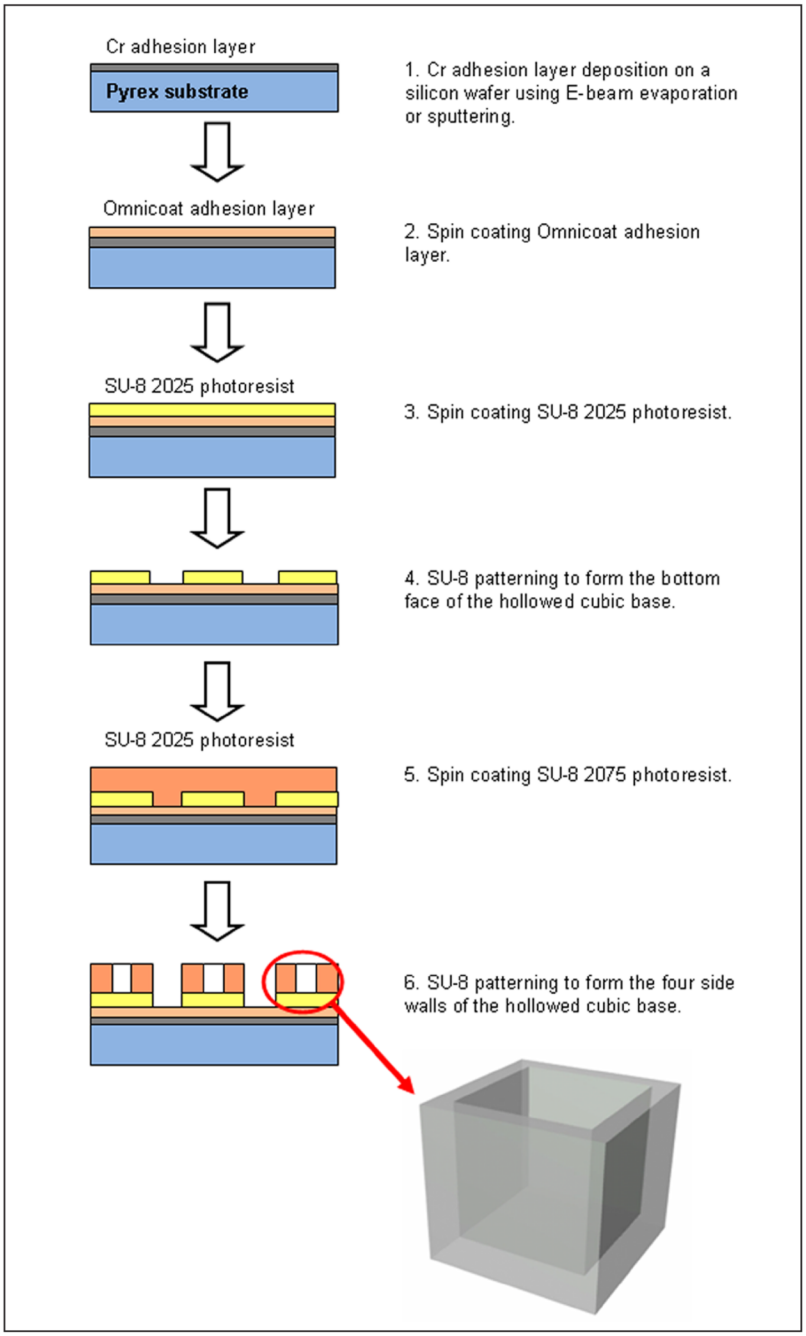

Figure 1.
Schematic outlining fabrication of the microcontainer base.

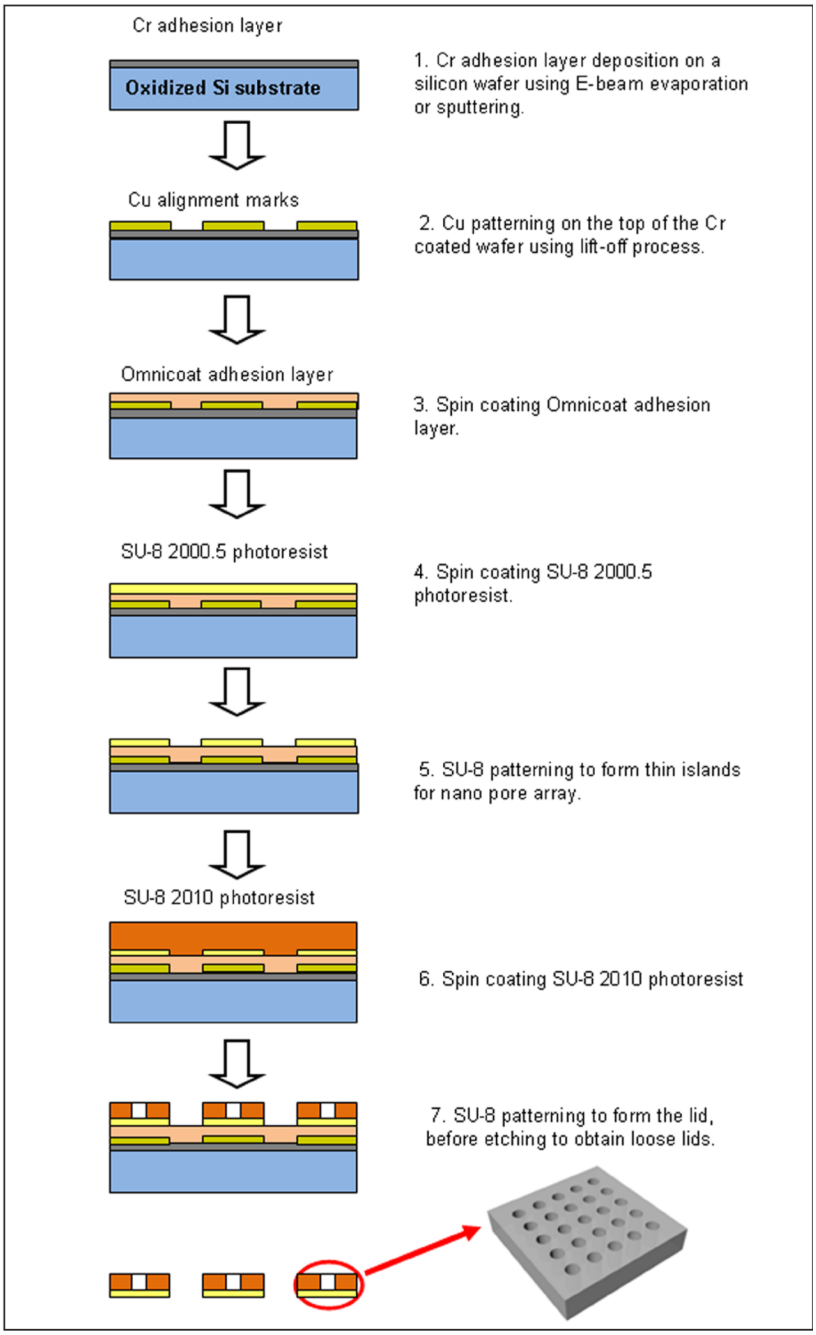

Figure 2.
Schematic outlining fabrication of the microcontainer lid.

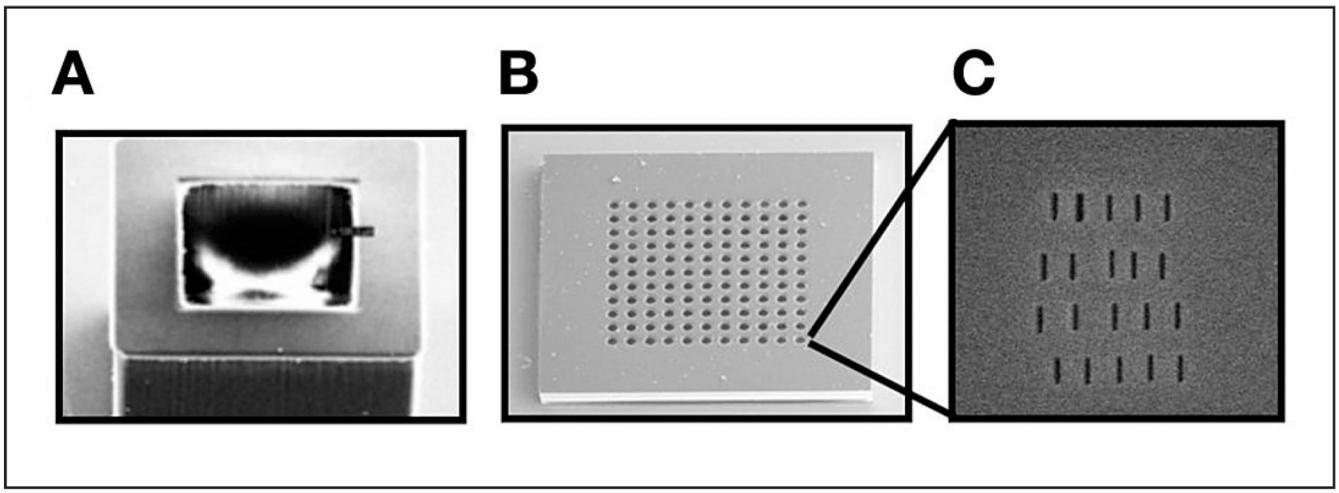

Figure 3.
Scanning electron microscope images of the microcontainer base **(A)** and lid **(B)** showing the 500-nm thin-membrane island structures. The thin membrane recessed within each island was milled with 25-nm slots using a focused ion beam **(C)**.

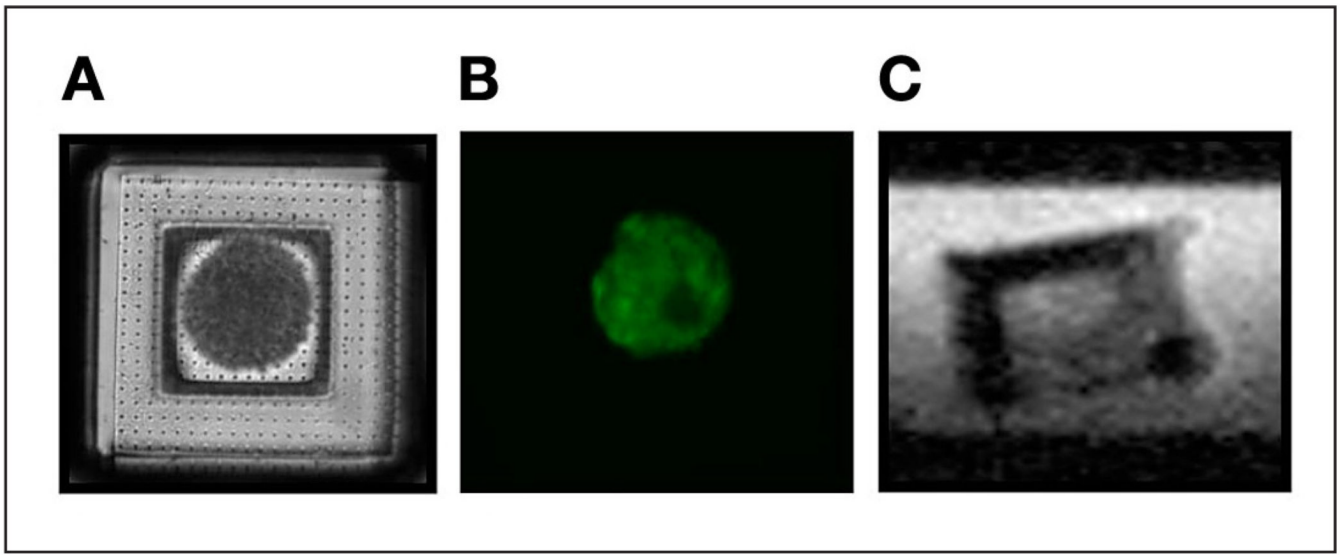

Figure 4.
The microcontainer base was loaded with an islet and closed with an optically transparent, nanoporous lid **(A)**. Viable cells were observed postencapsulation using fluorescence in the green channel **(B)**. Ultrahigh-resolution MRM demonstrated the ability to visualize the encapsulation volume of the microcontainer noninvasively **(C)**.

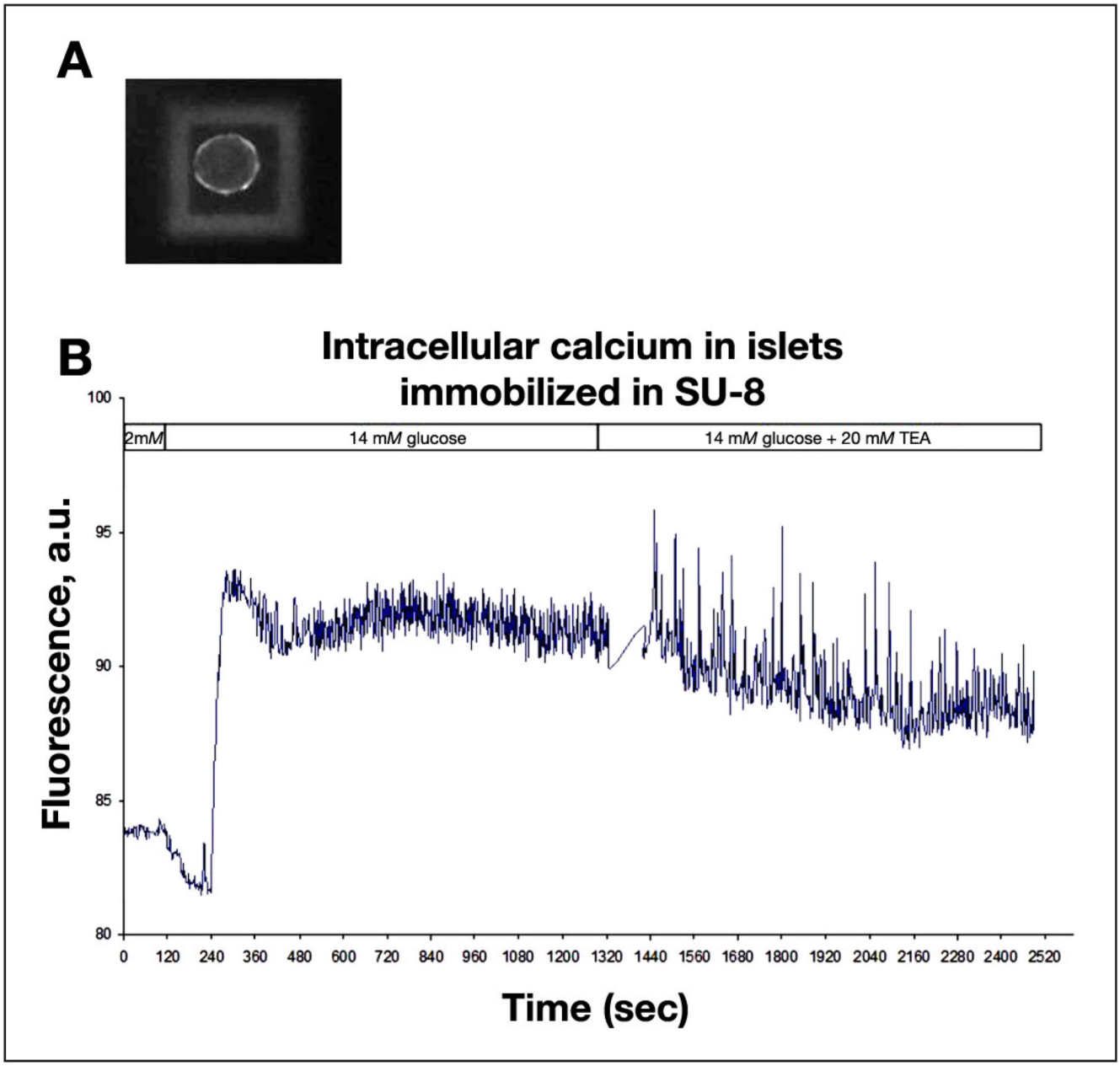

Figure 5.

For encapsulated islets, dynamic imaging of Ca^{2+} fluxes was performed with Fluo-4 **(A)**, and changes in the concentration of intracellular Ca^{2+} in response to glucose and TEA were quantified as seen in this representative trace **(B)**. a.u., arbitrary unit.